applied sciences

MDPI

Article

Performance Improvement of the Free-Space Optical Communication Link Using Spatial Diversity Reception-Assisted OFDM Signals

Yang Huang [1,2], Xinyi Zheng [1,2], Yufei Guo [1,2] and Shiming Gao [1,2,*]

[1] Centre for Optical and Electromagnetic Research, State Key Laboratory of Modern Optical Instrumentation, International Research Center for Advanced Photonics, Zhejiang University, Hangzhou 310058, China; 21930002@zju.edu.cn (Y.H.); zhengxinyi@zju.edu.cn (X.Z.); 22060531@zju.edu.cn (Y.G.)
[2] Ningbo Research Institute, Zhejiang University, Ningbo 315100, China
* Correspondence: gaosm@zju.edu.cn

Abstract: Orthogonal frequency division multiplexing (OFDM) technology is presented for use in free-space optical (FSO) communications accompanied by the spatial diversity reception. Using quadrature phase shift keying (QPSK) modulation formats, the OFDM signals show robustness to support high spectral efficiency and compatibility with the spatial diversity reception to improve receiver sensitivity. Compared with the single-carrier QPSK signal, the OFDM-QPSK signal with 64 sub-carriers can reduce the BER from 2.87×10^{-3} to 2.98×10^{-4} at the SNR of 6 dB. Using a two-aperture spatial diversity reception with OFDM, the BER can be reduced from 2.45×10^{-3} of a single receiver to 6.10×10^{-4} under moderate turbulence conditions. Under strong turbulence, the BER of the single receiver is 2.14×10^{-2}. It can be improved to 1.16×10^{-3} by using four-aperture receivers, and even 6.87×10^{-4} by using six-aperture receivers. The optimized aperture number should be selected according to channel conditions.

Keywords: free-space optical communications; orthogonal frequency division multiplexing; spatial diversity reception

Citation: Huang, Y.; Zheng, X.; Guo, Y.; Gao, S. Performance Improvement of the Free-Space Optical Communication Link Using Spatial Diversity Reception-Assisted OFDM Signals. *Appl. Sci.* **2022**, *12*, 6828. https://doi.org/10.3390/app12146828

Academic Editors: Habib Hamam and Amalia Miliou

Received: 7 June 2022
Accepted: 1 July 2022
Published: 6 July 2022

1. Introduction

Free-space optical (FSO) communication is widely employed in inter-satellite links, satellite-ground links, and communication between various flight platforms and terrestrial stations due to the advantages of high speed, high security, small equipment size, and no requirement of a spectrum license [1–4]. However, the atmospheric refractive index fluctuates randomly, resulting in an atmospheric turbulence effect [5]. It will severely deteriorate the laser beam and limit the FSO transmission distance or the communication bit rate. Techniques such as adaptive optics [6], aperture averaging [7], error control coding [8], and relaying [9] have been used to mitigate the effects of turbulence and improve the reliability of the FSO system.

For FSO transmission, higher speed signals suffer more from the influence of atmospheric turbulence. It will perform better if the data are separated into multiple low-speed consequences. Orthogonal frequency-division multiplexing (OFDM), which includes multiple orthogonal sub-carriers [10], can carry a high-speed data stream by dividing it into a series of low-speed sub-carrier signals. Furthermore, coherent modulation formats, such as binary phase shift keying and quadrature phase shift keying (QPSK), have better transmission performance in turbulence channels than intensity-modulated formats [11]. Coherent optical OFDM (CO-OFDM) has exhibited high spectral efficiency and strong anti-interference ability [12–14]. The complex OFDM series can be easily separated into real and imaginary components and modulated by an in-phase quadrature modulator

(IQM) [10]. As a result, it is entirely compatible with conventional coherent FSO communication systems. Using OFDM technology, an FSO communication link is experimentally demonstrated with a distance of 2.5 km and a rate of 10 Gbit/s, where a 3 dB receiver sensitivity improvement is obtained compared to OOK signals [15]. Moreover, a CO-OFDM-FSO scheme with quadrature amplitude modulation (QAM) signals has been proposed to significantly improve the transmission distance and data rate [13]. Furthermore, CO-OFDM with an optical receiving antenna array has been numerically predicted to realize a 20 Gbit/s FSO communication over 4500 km [16].

Diversity technologies, including spatial diversity, temporal diversity, polarization diversity, and wavelength diversity (or frequency diversity), are widely utilized to increase receiver sensitivity [17]. In principle, OFDM and diversity technology are compatible, and they can be used together to improve the link performance. The outage performance has been improved by using wavelength diversity in an OFDM-FSO system under E-Weibull channels [18]. The sensitivity has been predicted to improve by 6 dB with polarization diversity for an OFDM-FSO link [19]. Spatial diversity is a promising solution to suppress atmospheric turbulence [20]. In particular, spatial diversity reception with multiple receivers has a simple structure and does not need any extra change at the transmitter. The signals collected by all the receivers can be combined using digital signal processing (DSP) of linear combining algorithms, such as the selection combining (SC) algorithm, maximum ratio combining (MRC) algorithm, and equal gain combining (EGC) algorithm [21]. However, OFDM-FSO communications with spatial diversity reception are still limited. It is expected to improve the FSO receiving performance by combining the two kinds of technologies.

In this paper, we propose to detect the OFDM-QPSK signal using a spatial diversity receiver array in a FSO link in order to improve the receiving sensitivity. The turbulent channel is simulated by the phase screen method and the OFDM-QPSK signal is simulated using the Monte Carlo method to calculate the bit error rate (BER) and the constellation diagram. The sensitivity improvement of spatial diversity is evaluated by using multiple receivers.

2. System Structure and Channel Model

Figure 1 shows a schematic diagram of the proposed OFDM-based spatial diversity reception FSO communication system. At the transmitter, a radio frequency (RF) OFDM series carrying the initial data is modulated on an optical carrier through an IQM to generate the CO-OFDM signal, and it is launched into an atmospheric turbulence channel via a collimator. At the receiver, the signal is collected by multiple optical apertures, coupled into optical fibers, and demodulated by the coherent detectors. Then, these branched received signals are combined using an EGC algorithm after offline DSP processing.

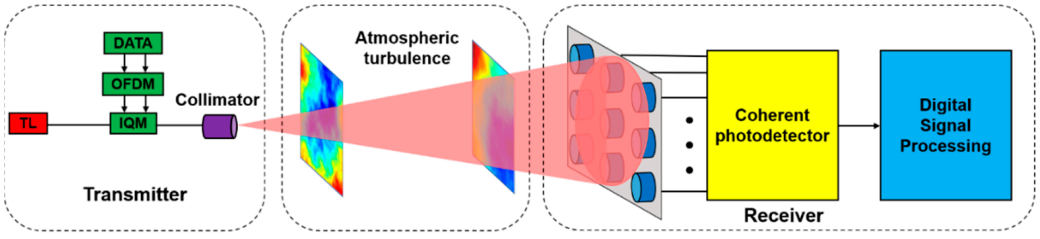

Figure 1. Schematic diagram of the spatial diversity reception FSO communication system using OFDM signals.

Figure 2a shows the schematic diagram of the modulating process of the CO-OFDM signal at the transmitter. The initial data are mapped into QPSK format, and then converted into a parallel sequence through serial-to-parallel conversion. The parallel sequence is modulated on the sub-carriers through inverse fast Fourier transform (IFFT), and a cyclic prefix (CP) is added. All sub-carriers are combined into an RF-OFDM-QPSK series through

parallel-serial conversion, which is modulated on the optical carrier through an IQM. Then, the CO-OFDM signal is sent to the atmospheric turbulence channel.

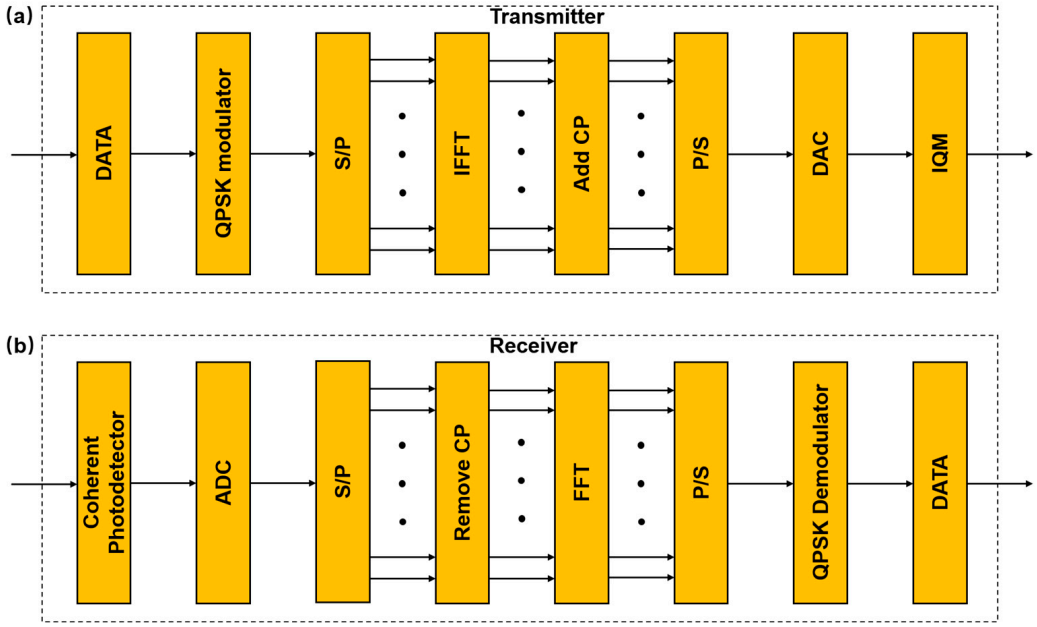

Figure 2. Processes of (**a**) the generation of the CO-OFDM-QPSK signal at the transmitter and (**b**) the demodulation of the signal at the receiver.

In the FSO communication system, the transmission of the signal will be influenced by the atmospheric turbulence to cause light attenuation, power jitter, and phase distortion. The FSO link can be expressed as

$$y = h \otimes s_{OFDM} + n, \tag{1}$$

where $s_{OFDM}(t) = \sum_{k=1}^{N} x_k exp(j2\pi f_k t)$ is the OFDM signal sent by the transmitter, N is the number of sub-carriers, f_k is the frequency of the kth sub-carrier, x_k is the complex data in the kth sub-carrier which is modulated in a QPSK format, y is the receiving signal at the receiver, n is the additive white Gaussian noise (AWGN), and h is the influence coefficient caused by the atmospheric turbulence channel. As shown in Figure 1, the OFDM-FSO system's performance can be evaluated by using a split-step beam propagation method based on phase screen theory [22]. The transmission distance L is divided into several segments, each of which has two parts: a vacuum transmission link of length Δz and a phase screen regardless of thickness. The effect of the atmospheric turbulence is superimposed on the optical carrier through the phase screen after the vacuum transmission. The phase screen is generated by the power spectrum inversion method. According to the von Karman model, the phase power spectral density is described as

$$\Phi(\kappa) = 0.033 C_n^2 \frac{\exp\left(-\kappa^2/k_m^2\right)}{\left(\kappa^2 + \kappa_0^2\right)^{11/6}}, \tag{2}$$

where $\kappa = 2\pi\left(f_x \hat{i} + f_y \hat{j}\right)$, $\kappa_m = 5.92/l_0$, $k_0 = 2\pi/L_0$, and l_0 and L_0 are the inner and outer scales of the turbulence, respectively. C_n^2 is the atmospheric refraction-index structure parameter, which can characterize the strength of atmospheric turbulence. The effect of the atmospheric turbulence on the CO-OFDM signal is simulated by transmitting it through a series of phase screens.

The optical signal is collected by multiple apertures at the receiver after introducing the AWGN noise. As shown in Figure 2b, the CO-OFDM signal is down-converted to RF-OFDM by coherent photodetectors. After compensating for the frequency offset and the

phase noise of each receiver branch signal, and then sampled through an analog-to-digital converter. The initial data are reconstructed through serial-to-parallel conversion, CP removal, fast Fourier transform (FFT), parallel-to-serial conversion, and QPSK demodulation. The EGC algorithm is used to combine them for its high diversity gain and easy combining process [23,24]. The weight coefficient of each branch is selected as 1, and the phase alignment is realized by calculating the relative phase between each channel and the reference channel with the largest SNR [25]. Finally, the constellation diagram and BER curves are obtained.

3. Simulation Results and Discussion

3.1. Improvement Based on OFDM

In the simulation, the initial values of the used parameters are shown in Table 1. The optical carrier output from the transmitter was supposed to satisfy the Gaussian distribution. The transmission length was divided into 10 segments with the equal spacing, and one phase screen was placed at the end of each segment. In total, 1000 samples were collected to investigate the atmospheric turbulence effect on laser transmission. Figure 3a–c show the normalized optical intensity variations under weak, moderate, and strong turbulence conditions. With the turbulence strengthened, the fluctuations of the optical intensity are enhanced. The variance of the optical intensities is 0.0088, 0.2104, and 0.4898 for weak, moderate, and strong turbulences, respectively.

Table 1. Simulation parameter values.

Symbol	Value
Wavelength, λ	1550 nm
Link distance, L	1000 m
Phase screen size	0.5 m × 0.5 m
Inner scale, l_0	0
Outer scale, L_0	100 m
Refractive-index structure parameters, C_n^2	5×10^{-15} $m^{-2/3}$ (weak turbulence) 5×10^{-14} $m^{-2/3}$ (moderate turbulence) 5×10^{-13} $m^{-2/3}$ (strong turbulence)

The performance of the OFDM-FSO transmission link was evaluated in an atmospheric turbulence channel. A 20 Gbit/s pseudo-random bit sequence (PRBS) was mapped to the QPSK modulation format, and then loaded onto 64 sub-carriers. Another 8 sub-carriers were used as the CP to eliminate the inter-symbol interference (ISI). Finally, the IFFT with a size of 128 was used to convert the data into an OFDM signal. Figure 4 shows the BER curve of this OFDM-QPSK signal in the turbulence channel with the refractive-index structure parameters C_n^2 of 5.0×10^{-15} $m^{-2/3}$, where the BER of the single carrier QPSK (SC-QPSK) signal was also simulated for comparison. The BER of the OFDM-QPSK signal is much lower than that of the SC-OFDM signal without sub-carriers. At the SNR of 6 dB, the achieved BERs of the SC-QPSK and the OFDM-QPSK signals are 2.87×10^{-3} and 2.98×10^{-4}, which are efficiently reduced. Figure 5a,b show the constellation diagrams of the OFDM-QPSK and the SC-QPSK signal at the same SNR of 6 dB. Their error vector magnitudes are 0.3481 and 0.4903, which means that the OFDM-QPSK signal has a better quality than the SC-QPSK signal.

Figure 6 shows the BER of the OFDM-QPSK signal as a function of the SNR under different turbulence conditions, as shown in Table 1. At the SNR of 6 dB, the BER of the OFDM signal under weak, moderate, and strong turbulences is 2.98×10^{-4}, 2.45×10^{-3}, and 2.14×10^{-2}, respectively. The transmission quality degrades as the turbulence strengthens. In Figure 6, the BER curves become flat under moderate and strong turbulence. The reason may be that the degradation caused by the turbulence is too heavy to be fully compensated by the DSP. The signal quality cannot be further improved even though the SNR increases.

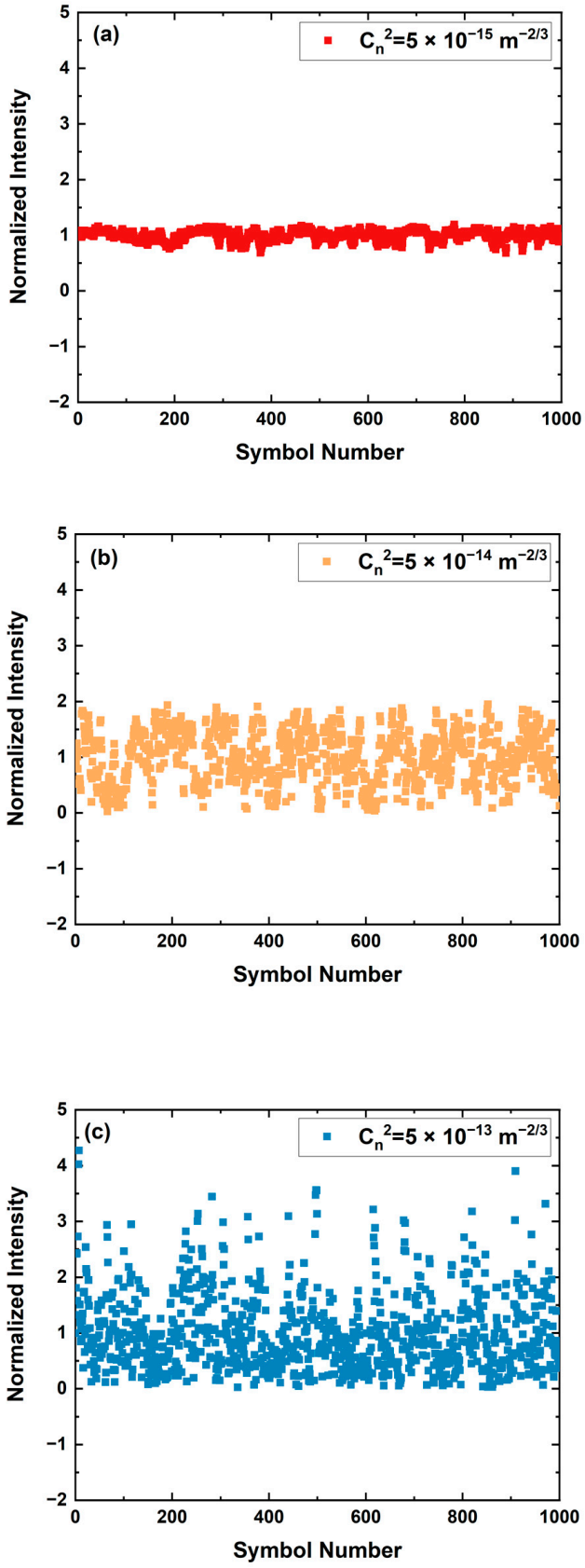

Figure 3. Normalized optical intensity variations under (**a**) weak turbulence, (**b**) moderate turbulence and (**c**) strong turbulence.

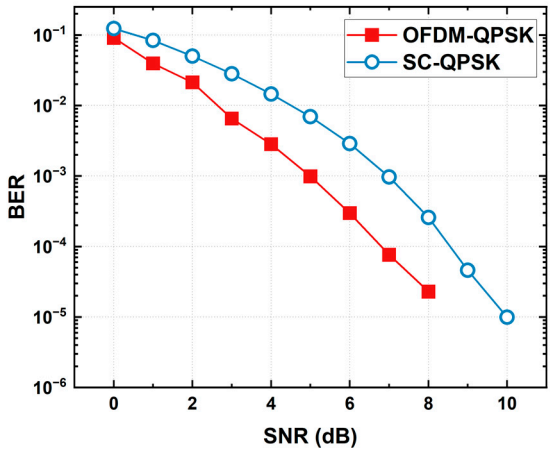

Figure 4. BER curves of the OFDM-QPSK signal and the SC-QPSK signal.

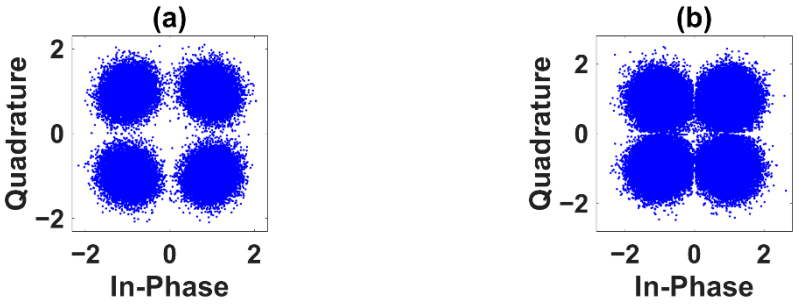

Figure 5. Constellation diagrams of (**a**) OFDM-QPSK and (**b**) and SC-QPSK at the SNR of 6 dB.

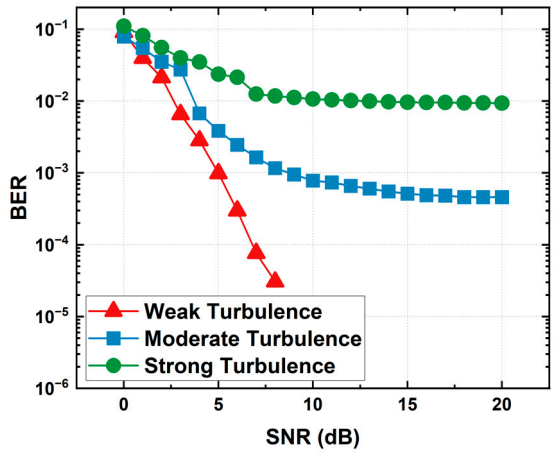

Figure 6. BER curves of the OFDM signal under different turbulence conditions.

3.2. Improvement Using Spatial Diversity

The spatial diversity reception technology is adopted to further improve the receiver sensitivity. Figure 7 depicts the BER curve as a function of the SNR with different aperture numbers of receivers. Figure 7a–c show the weak, moderate, and strong turbulences, respectively. Here, 1R, 2R, 4R, and 6R represent the aperture number 1, 2, 4, and 6, respectively. In the case of weak turbulence shown in Figure 7a, the system performance cannot be further improved by increasing the aperture number since the sensitivity of a single receiver is sufficient. In the moderate turbulence (see Figure 7b), the performance of two-aperture spatial diversity is much better than the single receiver. At the SNR of 6 dB, the required BER drops from 2.45×10^{-3} to 6.10×10^{-4} if the two-aperture receiver array is used instead of the single receiver. By further increasing the aperture number to four, the

BER is further reduced to 3.89×10^{-4} by using four-aperture receivers. Under the strong turbulence, the BER cannot be reduced below 0.01 using a single receiver, even when the SNR is increased to as high as 20 dB. Using two-aperture spatial diversity reception, the BER can reach approximately 1×10^{-3}. While four-aperture receivers are adopted, the BER is reduced to 1×10^{-4} when the SNR is about 10 dB. At the SNR of 6 dB, the BERs are 2.14×10^{-2}, 6.23×10^{-3}, 1.16×10^{-3}, and 6.87×10^{-4} for the single receiver, two-aperture receivers, four-aperture receivers, and six-aperture receivers, respectively. It can be seen that the FSO link performance of the OFDM-QPSK signal is effectively improved using the spatial diversity reception.

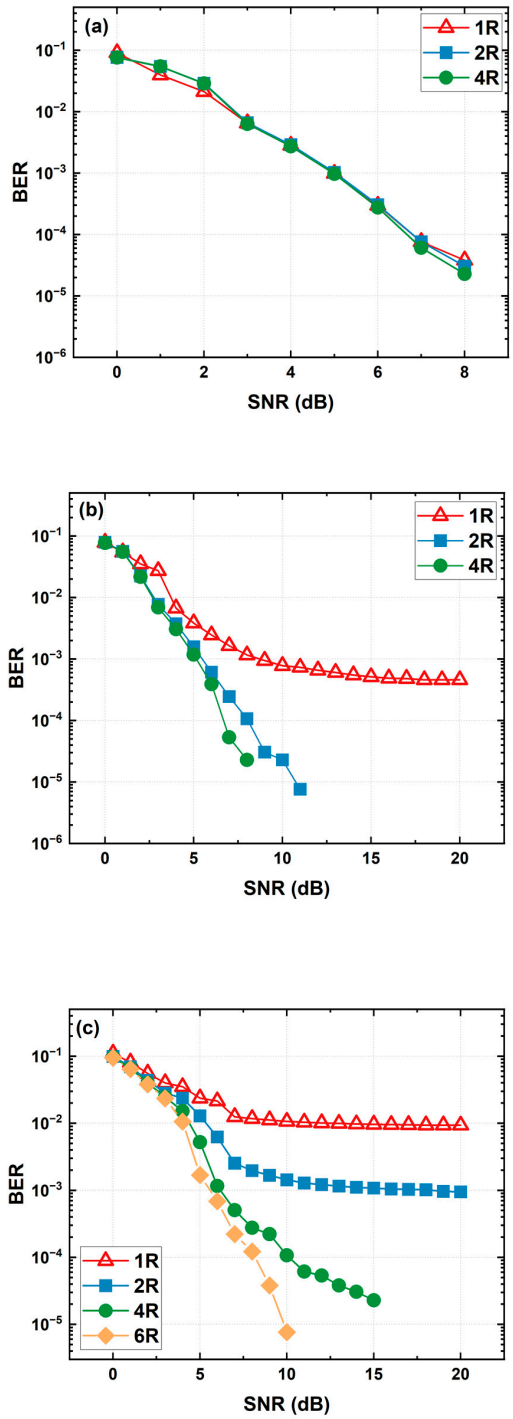

Figure 7. BER curves of the spatial diversity reception under different turbulence conditions: (**a**) weak turbulence, (**b**) moderate turbulence, and (**c**) strong turbulence.

The above analysis shows that the OFDM-QPSK link performance can be effectively improved by using spatial diversity, but the improvement becomes limited as the receiver aperture number increases. Therefore, it is reasonable to consider an optimal aperture number of receivers under the requirement of a certain BER. Here, a requirement for the number of apertures is proposed, where the maximum BER of 1×10^{-3} is permitted when the signal SNR is 6 dB. In this way, Figure 8 shows the required aperture number of receivers under different turbulent conditions. As turbulence strength increases, the required aperture number of receivers increases accordingly. When the turbulence is weak, a single receiver is sufficient. For the moderate turbulences (such as C_n^2 is 5×10^{-14} $m^{-2/3}$ and 1×10^{-13} $m^{-2/3}$, corresponding to the Rytov coefficients of 0.99 and 1.99, respectively), 2–4 aperture receivers are needed to satisfy the BER requirement. Moreover, at least 6 aperture receivers are required to keep the BER below 1×10^{-3} under strong turbulence with C_n^2 of 5×10^{-13} $m^{-2/3}$ (the Rytov coefficient is 9.95). In practical applications, the appropriate aperture number of receivers should be selected according to the channel conditions.

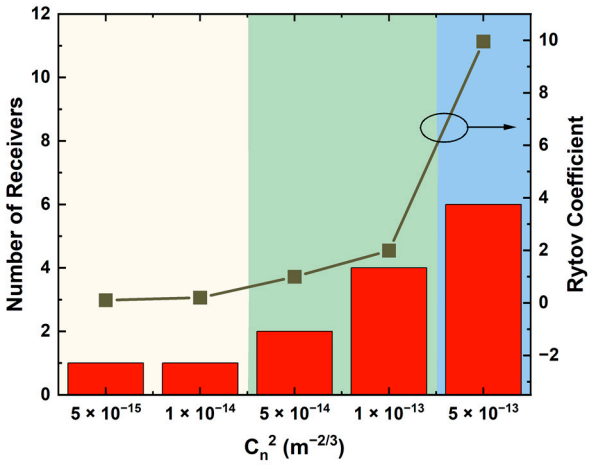

Figure 8. Required aperture number of receivers for the BER below 1×10^{-3} at the SNR of 6 dB.

4. Conclusions

An OFDM-QPSK transmission link accompanied by the spatial diversity reception was proposed to improve the performance of FSO communications. The OFDM signal exhibited better performance than the single-carrier signal, and the BER was reduced from 2.87×10^{-3} to 2.98×10^{-4} at an SNR of 6 dB by using the OFDM-QPSK signal instead of the SC-QPSK signal. The receiving sensitivity was further improved by the spatial diversity reception. Under moderate turbulence, the BER decreased from 2.45×10^{-3} to 6.10×10^{-4} at an SNR of 6 dB by using two-aperture receivers. Under strong turbulence, the BER was reduced to 6.87×10^{-4} by using six-aperture receivers from 2.14×10^{-2}. More aperture numbers are required with turbulence strengthening, and it should be selected according to the used channel conditions.

Author Contributions: Y.H. contributed to the paper in terms of methodology, program, visualization, and data analysis and paper draft. X.Z. and Y.G. contributed to the paper in terms of investigation, resources, and project administration. S.G. contributed to the paper in terms of conceptualization, supervision, review, and editing. All authors have read and agreed to the published version of the manuscript.

Funding: This research was funded by the National Natural Science Foundation of China (61875172, U2141231), the Zhejiang Provincial Natural Science Foundation of China (LD19F050001), and the National Key Research and Development Program of China (2019YFB2205202).

Institutional Review Board Statement: Not applicable.

Informed Consent Statement: Not applicable.

Data Availability Statement: Not applicable.

Acknowledgments: The author acknowledges the valuable comments of the reviewers.

Conflicts of Interest: The authors declare no conflict of interest.

References

1. Kaushal, H.; Kaddoum, G. Optical communication in space: Challenges and mitigation techniques. *IEEE Commun. Surv. Tutor.* **2017**, *19*, 57–96. [CrossRef]
2. Henniger, H.; Wilfert, O. An introduction to free-space optical communications. *Radioengineering* **2010**, *19*, 203–212.
3. Chan, V.W.S. Free-space optical communications. *J. Lightwave Technol.* **2006**, *24*, 4750–4762. [CrossRef]
4. Gismalla, M.S.M.; Abdullah, M.F.L.; Sami, M.; Shah, N.S.M.; Das, B.; Qasim, A.A. Effect of Optical Attocells Deployment on the RMSD Spread in Indoor Visible Light Communication Systems. In Proceedings of the 2020 International Conference on Information Science and Communication Technology (ICISCT), Karachi, Pakistan, 8–9 February; pp. 1–6. [CrossRef]
5. Wang, L.; Wang, J.; Tang, X.; Chen, H.; Chen, X. Performance analysis of a spatial diversity coherent free-space optical communication system based on optimal branch block phase correction. *Opt. Express* **2022**, *30*, 7854–7869. [CrossRef]
6. Liu, W.; Yao, K.; Huang, D.; Lin, X.; Wang, L.; Lv, Y. Performance evaluation of coherent free space optical communications with a double-stage fast-steering-mirror adaptive optics system depending on the greenwood frequency. *Opt. Express* **2016**, *24*, 13288–13302. [CrossRef] [PubMed]
7. Elsayed, E.E.; Yousif, B.B. Performance enhancement of the average spectral efficiency using an aperture averaging and spatial-coherence diversity based on the modified-PPM modulation for MISO FSO links. *Opt. Commun.* **2020**, *463*, 125463. [CrossRef]
8. Gupta, R.; Kamal, T.S. Performance analysis of OFDM based FSO communication system with TCM codes. *Optik* **2021**, *248*, 168141. [CrossRef]
9. Erdogan, E.; Altunbas, I.; Kabaohlu, N.; Yanikomeroglu, H. A cognitive radio enabled RF/FSO communication model for aerial relay networks: Possible configurations and opportunities. *IEEE Open J. Veh. Technol.* **2020**, *2*, 45–53. [CrossRef]
10. Shieh, W.; Bao, H.; Tang, Y. Coherent optical OFDM: Theory and design. *Opt. Express* **2008**, *16*, 841–859. [CrossRef]
11. Gismalla, M.S.M.; Abdullah, M.F.L.; Ahmed, M.S.; Mabrouk, W.A.; AL-Fadhali, N.; Saeid, E.; Supa'at, A.S.M.; Das, B. Design and analysis of different optical attocells deployment models for indoor visible light communication system. *Int. J. Integr. Eng.* **2021**, *13*, 253–264. [CrossRef]
12. Jansen, S.; Borne, D.; Adhikari, S. Past, Present and Future of Optical OFDM. In Proceedings of the Communications and Photonics Conference and Exhibition (ACP, 2009), Shanghai, China, 2–6 November 2009; pp. 1–5. [CrossRef]
13. Sharma, V.; Sushank. High speed CO-OFDM-FSO transmission system. *Opt. Int. J. Light Electron. Opt.* **2014**, *125*, 1761–1763. [CrossRef]
14. Shieh, W.; Athaudage, C. Coherent optical orthogonal frequency multiplexing. *Electron. Lett.* **2006**, *42*, 587–589. [CrossRef]
15. Cvijetic, N.; Qian, D.; Wang, T. 10Gb/s Free-Space Optical Transmission Using OFDM. In Proceedings of the Optical Fiber Communication Conference (p. OThD2), Optical Society of America, San Diego, CA, USA, 24–28 February 2008. [CrossRef]
16. Khichar, S.; Inanyia, P. Evaluation of performance of Is-OWC OFDM system with spatial diversity. *Opt. Wirel. Technol.* **2020**, *2020*, 49–55.
17. Mohaisen, M.; Wang, Y.; Chang, K. Multiple antenna technologies. *arXiv* **2009**, arXiv:0909.3342. [CrossRef]
18. Wang, Y.; Zhu, L.; Feng, W. Performance study of wavelength diversity serial relay OFDM FSO system over exponentiated Weibull channels. *Opt. Commun.* **2021**, *478*, 126470. [CrossRef]
19. Islam, M.; Majumder, S. Analytical evaluation of the cross-polarization induced crosstalk on BER performance of an OFDM FSO link with polarization diversity. *Opt. Commun.* **2020**, *474*, 126095. [CrossRef]
20. Abaza, M.; Mesleh, R.; Mansour, A.; Aggoune, E. Spatial Diversity for FSO Communication Systems over Atmospheric Turbulence Channels. In Proceedings of the 2014 IEEE Wireless Communications and Networking Conference (WCNC), Istanbul, Turkey, 6–9 April 2014; pp. 382–387. [CrossRef]
21. Abadi, M.; Ghassemlooy, Z.; Smith, D.; Ng, W.; Zvanovec, S. Comparison of Different Combining Methods for Space-Diversity FSO Systems. In Proceedings of the 9th IEEE/IET International CSNDSP14 IEEE, Manchester, UK, 23–25 July 2014; pp. 1023–1028. [CrossRef]
22. Yu, Z.; Cai, R.; Wu, Z.; He, H.; Jiang, H.; Feng, X.; Zheng, A.; Chen, J.; Gao, S. Performance evaluation of direct-detection coherent receiver array for free-space communications with full-link simulation. *Opt. Commun.* **2020**, *454*, 124520. [CrossRef]
23. Karagiannidis, G.; Zogas, D.; Sagias, N.; Kotsopoulos, S.; Tombras, G. Equal-gain and maximal-ratio combining over nonidentical Weibull fading channels. *IEEE Trans. Wirel. Commun.* **2005**, *4*, 841–846. [CrossRef]
24. Sun, J.; Huang, P.; Yao, Z.; Guo, J. Adaptive digital combining for coherent free space optical communications with spatial diversity reception. *Opt. Commun.* **2019**, *444*, 32–38. [CrossRef]
25. Zheng, A.; Huang, Y.; Gao, S. Modeling and spatial diversity-based receiving improvement of in-flight UAV FSO communication links. *Appl. Sci.* **2021**, *11*, 6365. [CrossRef]